Intensity and polarization of thermal radiation of three-dimensional rain cells in the microwave band

Ya. A. Ilyushin, B. G. Kutuza, A. A. Sprenger, and V. G. Merzlikin

Intensity and Polarization of Thermal Radiation of Three-Dimensional Rain Cells in the Microwave Band

Ya. A. Ilyushin[1,2,a)], B. G. Kutuza[2], A. A. Sprenger[1] and V. G. Merzlikin[3,4]

[1] *Moscow State University, Physical Faculty Leninskie gory, ulitza Lebedeva, GSP-2, 119992, Moscow, Russia*
[2] *Kotel'nikov Institute of Radio Engineering and Electronics, Mokhovaya st., 11-7, 125009, Moscow, Russia*
[3] *Plekhanov Russian University of Economics, Dept. of Technical and Economic Systems, Moscow, Russia*
[4] *Moscow State University of Mechanical Engineering (MAMI), Physics Dept., Moscow, Russia*

[a)] Corresponding author: ilyushin@phys.msu.ru

Abstract. In the present paper, the problems of formation and observation of spatial and angular distribution of thermal radiation of raining atmosphere in the millimeter wave band are addressed. Radiative transfer of microwave thermal radiation in three-dimensional dichroic medium is simulated numerically. Governing role of three dimensional cellular inhomogeneity of the precipitating atmosphere in the formation of thermal radiation field is shown.

INTRODUCTION

Investigation of atmospheric precipitation with the space borne instrumental observations is one of most important problems in remote sensing. First time, a possibility of retrieval of rain intensity from microwave observations has been demonstrated in 1968 with the results of Cosmos-243 space-borne experiment [1]. Rain precipitation zones over the sea have been identified and rain intensity was estimated from radio brightness temperatures at wavelengths 0.8, 1.35 and 3.2 cm.

Further development of techniques of space-borne precipitation observations is related to the DMSP satellite with microwave radiometer SSM/I [2] on board, operating in the wavelength band 0.35 - 1.6 cm. Precipitation zones have been determined as low radio brightness areas at 0.35 cm wavelength because of high multiple scattering albedo of big rain droplets. Also, microwave radiometry of rain precipitation has been performed from TRMM satellite. At present, GPM (Global Precipitation Mission) project is under development.

Due to this and other directions of research, interaction of microwave radiation with precipitations and clouds of various types is now extensively studied [3-13]. Many of them consist of non-spherical particles, having prevalent orientation like falling raindrops. In contrast to macroscopically isotropic media, in these media dichroism plays a key role in generation and propagation of the radiation. These effects together with spatial inhomogeneity of the medium as well as underlying surface require consideration of radiation fields in three-dimensional inhomogeneous dichroic media. However, to the authors' knowledge, only a few numerical studies of vectorial radiative transfer in three dimensional anisotropic scattering media are published [12]. This paper is motivated by the need in theoretical assessments of intensity and polarization of thermal radiation of rain precipitation, observed by a space-borne microwave radiometer.

PHYSICAL MODEL OF RADIATIVE CHARACTERISTICS OF THE MEDIUM

In the present study, the three dimensional cubic rain cell model [14] is investigated and compared to the flat layered slab model of the raining atmosphere. Following to [12], we chose cubic rain cell model ($3 \times 3 \times 3$km), uniformly filled with falling raindrops. Physical (thermodynamic) temperature in the atmosphere is non-uniform and decreases with height T2 = (300 - 7z) K, where z is a height in km.

Radiation Processes in the Atmosphere and Ocean (IRS2016)
AIP Conf. Proc. 1810, 040003-1–040003-4; doi: 10.1063/1.4975505
Published by AIP Publishing. 978-0-7354-1478-5/$30.00

Underlying surface is approximated with horizontal flat nearly isotropically radiating gray surface with partial lambertian reflection. Thermal radiative emission of the heated underlying surface is slightly vertically polarized [15].

Underlying surface in the flat layer model is black (lambertian reflection coefficient R = 0) of gray (R = 0.25) surface. In the cubic rain cell model, underlying surface within the square bottom of the cell is also black or gray as well as in the uniform slab model. Outside the bottom surface, it is totally black (R = 0). Temperature dependence of dielectric properties of liquid water has been ignored, thus the properties of the medium have been assumed to be constant in the whole height range of the cell or the slab. All the dielectric properties of the water have been evaluated for T = 0∘C.

Complex dielectric permittivity of the liquid water obeys the Debye formula [16,17]. Static dielectric permittivity if the liquid water is described by the known approximate formula [15]. Non-spherical falling raindrops with a reasonable degree of approximation can be regarded to be oblate spheroids with vertically oriented rotational axis of symmetry. Ratio of axes of the spheroid depends on the raindrop size [18]. Raindrop sizes are distributed statistically according to Marshall-Palmer distribution [19]. Extinction and absorption matrices of the spheroidal particles of fixed orientation can be evaluated by public available T-matrix codes [20].

RADIATIVE TRANSFER IN THE ANISOTROPIC SCATTERING MEDIUM

Spatial and angular distribution of the intensity and polarization of thermal radiation in the rain precipitation medium is governed by the vectorial radiative transfer equation

$$\left(\vec{\Omega}\cdot\nabla\right)I\left(\vec{r},\vec{\Omega}\right) == \hat{\sigma}_{\varepsilon} I\left(\vec{r},\vec{\Omega}\right) + \overline{\sigma}_{a} B_{\lambda}\left(T_{2}(z)\right) + \frac{1}{4\pi}\int_{4\pi} x\left(\vec{\Omega},\vec{\Omega}'\right) I\left(\vec{r},\vec{\Omega}'\right) d\vec{\Omega}' \quad , \tag{1}$$

where $\vec{\Omega} = (\mu_x, \mu_y, \mu_z)$ - unit vector of arbitrary direction, $I\left(\vec{r},\vec{\Omega}\right) = \{I, Q, U, V\}$ -- Stokes parameters vector of polarized radiation, $\hat{\sigma}_{\varepsilon} = \hat{\sigma}_{\varepsilon}\left(\vec{\Omega}\right)$-- extinction matrix of polarized radiation in the medium, $\overline{\sigma}_{a}$ - vector of true absorption in the medium, $x\left(\vec{\Omega},\vec{\Omega}'\right)$- scattering matrix, $B_{\lambda}(\cdot)$- Planck black body radiation function. Formulae for evaluation of the true absorption vector components σ_a can be found, e.g., in [19].

In the millimeter wave band at temperatures about 300 K, typical for lower terrestrial atmosphere, Planckian black body radiation at the given wavelength is roughly proportional to the black body temperature (Rayleigh-Jeans law). This allows the Stokes parameters to be expressed immediately through the equivalent black body temperature (radio brightness temperature).

Boundary problem for the vectorial radiative transfer equation in 3D cubic rain cell consists of the equation (1) and boundary conditions for the incoming radiation at all the cube sides. Boundary condition on the top surface of the rain cell is just zero boundary condition for the incoming radiation. Boundary conditions on side walls and bottom of the rain cell account for the thermal radiation coming from the heated underlying surface and lossy gray surrounding atmosphere [14].

SIMULATION RESULTS

There has been performed large series of numerical simulations of microwave radiative transfer in slab layer and rectangular rain cell with different parameters (rain intensity, additional atmospheric absorption and underlying surface diffuse reflection coefficient) [21]. Typical simulated three-dimensional views of rain cell are shown in Figures 1,2.

Linear polarization degree of radiation for cell model (the 2nd Stokes parameter Q) is two or three times smaller than the corresponding value for slab medium model. Liquid water clouds, water vapor and oxygen, and weak diffuse reflection of the radiation from the underlying surface does not significantly impact these angular dependencies and relations between them. Indeed, distributions of the polarization parameters Q and U of the cell with absolutely black underlying surface (the Figure 1) do not differ significantly from the ones of partially reflective underlying surface (the Figure 2). On the other hand, the radio brightness temperature (the intensity, Stokes parameter I, the Figure 1) is notably impacted by the Lambertian reflectivity of the surface beneath the cell. Roughly speaking, the cold cell bottom is partially seen through the cell’s side walls.

From the simulation results it turns out that geometrical model of isolated cubic rain cell, which is rough simplification of true inhomogeneous distribution of realistic rain precipitation in the atmosphere, showed inhomogeneous distribution of thermal radiation intensity and polarization. It worth also noting appearance of the third Stokes parameter U, which is observed experimentally [18], in the simulated radiative field of the rain cell. This parameter U, which characterizes the tilt angle of the radiation polarization plane, does not appear in the layered slab medium model with the vertically oriented axes of the rotationally symmetric particles (raindrops). The polarization plane of the thermal radiation of layered slab medium can be tilted, if the rotational axes of the raindrops are systematically tilted themselves [18]. The mechanisms of such raindrops' axes inclination (wind etc.) are, however, still questionable, and are out of the scope of this paper. The rain cell model is therefore able to qualitatively explain the polarization plane tilt without the tilted raindrops hypothesis being involved.

Thus, radiative transfer simulations with the cubic cell model discovered limitations of flat layered slab model, which still largely remains the basic and most used computational model in atmospheric radiation studies.

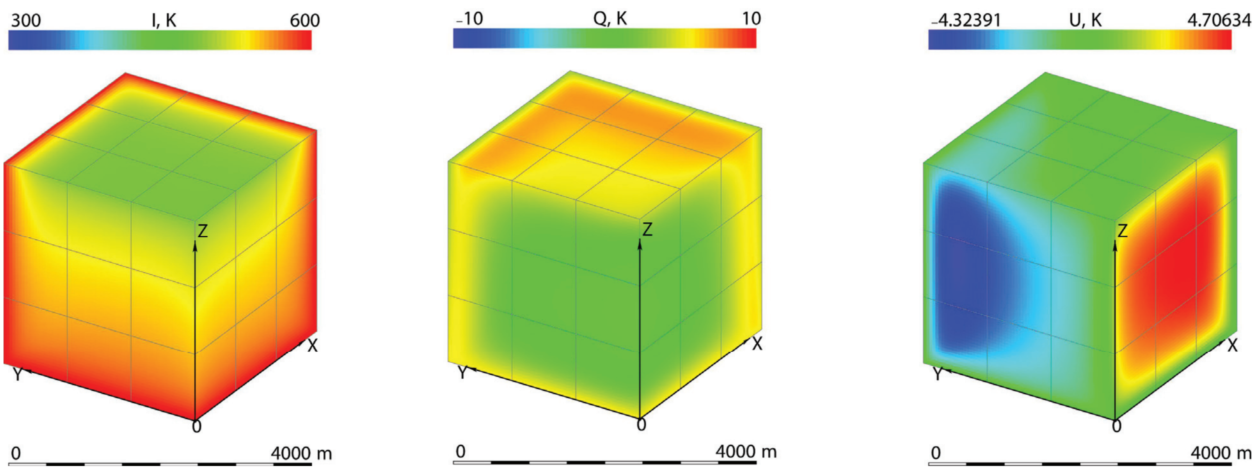

FIGURE 1. 3D rain cell view projection. Wave length λ = 3 mm, rain intensity 20 mm/h, lambertian reflectance R = 0.

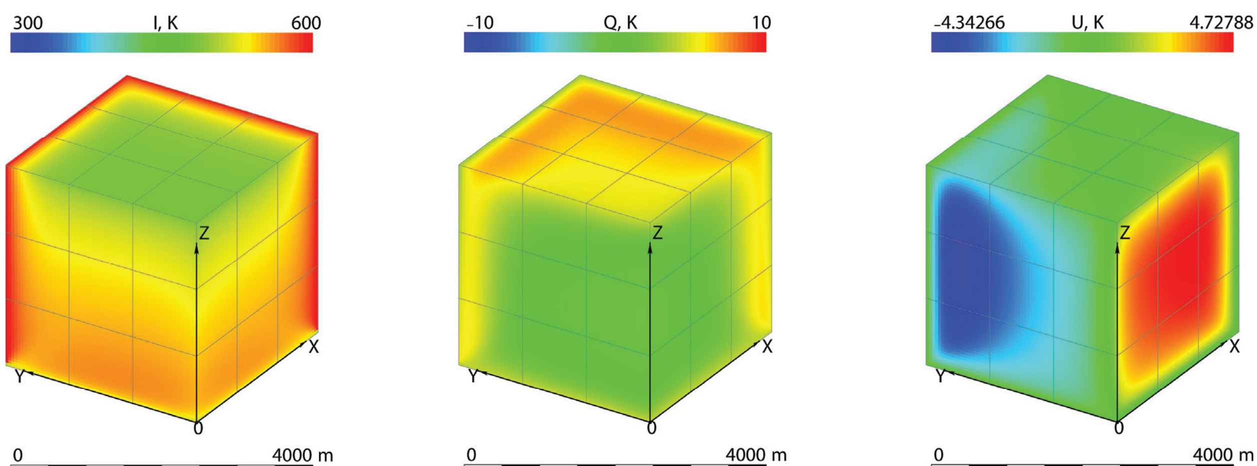

FIGURE 2. 3D rain cell view projection. Wave length λ = 3 mm , rain intensity 20 mm/h, lambertian reflectance R = 0.25

CONCLUSIONS AND FINAL REMARKS

In the study presented here, extensive numerical simulations of thermal radiation field in precipitating atmosphere in millimeter wave band have been performed. Commonly used uniform slab model of rain atmosphere is validated against three-dimensional rain cell model. Simulation results for intensity and polarization of the thermal radiation have been presented and interpreted. Calculations confirm linear polarization of rain cell thermal radiation, which is about 2-3 K in average over observable surface area of the cell.

Spatial resolution of existing space-borne millimeter wave radiometers is now about 15-20 km, which well exceeds typical size of the rain cell. Thus, several rain cells with different rain intensity are typically covered by the radiometer's field of view. Because of large contribution of underlying surface to the intensity and polarization, it is not possible to separate it from the contribution of precipitation (rain). To do that, one needs to improve significantly spatial resolution of the radiometer, to make its field of view comparable to or smaller than typical rain cell dimension. This can be achieved with millimeter wave synthetic aperture interferometer, or with large size antenna systems with capability of electrical or mechanical scanning.

ACKNOWLEDGEMENTS

This study is partially supported by Russian Fundamental Research Fund with the grants 13-02-12065 ofi-m and 15-02-05476. The authors are grateful to the administration of the Scientific Research Computing Center of the Moscow State University for granting the access to the parallel computing system SKIF-GRID "Lomonosov".

REFERENCES

1. E. Basharinov, A. S. Gurvich, and S. T. Egorov, *Radio Emission of the Earth as a Planet* (Nauka, Moscow, 1974).
2. R. Spencer, H. Goodman, and R. Hood, J. Ocean. Technol. **6**, 254-273 (1989).
3. B. G. Kutuza and M. T. Smirnov, Issledovanie Zemli iz Kosmosa **1**, 76-83 (1980).
4. S. P. Gagarin and B. G. Kutuza, IEEE Journal of Oceanic Engineering **8**, 62-70 (1983).
5. B. G. Kutuza and M. T. Smirnov, Digest - International Geoscience and Remote Sensing Symposium (IGARSS) **1**, 193-194 (1991).
6. A. Hornbostel, A. Schroth, A. Sobachkin, B. G. Kutuza, A. Evtuchenko, and G. K. Zagorin, International Geoscience and Remote Sensing Symposium (IGARSS) **4**, 2078-2080 (1999).
7. L. Roberti, J. Haferman, and C. Kummerow, Journal of Geophysical Research **99,** 16707-16718 (1994).
8. B. G. Kutuza, G. K. Zagorin, A. Hornbostel, and A. Schroth, Radio Science **33**, 677-695 (1998).
9. T. J. Jackson, A. Y. Hsu, A. Shutko, Y. Tishchenko, B. Petrenko, B. G. Kutuza, and N. Armand, International Journal of Remote Sensing **23**, 231-248 (2002).
10. B. G. Kutuza, Radio Science **38**, MAR12/1-MAR12/7 (2003).
11. B. G. Kutuza and G. K. Zagorin, Radio Science **38**, MAR20/1-MAR20/7 (2003).
12. A. Battaglia, C. Davis, C. Emde, and C. Simmer, Journal of Quantitative Spectroscopy and Radiative Transfer **105**, 55-67 (2007).
13. V. K. Volosyuk, Y. V. Gulyaev, V. F. Kravchenko, B. G. Kutuza, V. V. Pavlikov, and V. I. Pustovoit, Journal of Communications Technology and Electronics **59**, 97-118 (2014).
14. Y. A. Ilyushin and B. G. Kutuza, Izvestiya - Atmospheric and Ocean Physics **52**, 74-81 (2016).
15. F. T. Ulaby, R. K. Moore, and A. K. Fung, *Microwave remote sensing: Active and passive*, Vol. 1 (Reading, MA:Addison-Wesley, 1981).
16. A. E. Basharinov and B. G. Kutuza, Izv. Vyssh. Uchebn. Zaved., Radiofiz. **17**, 52-57 (1974).
17. A. Akvilonova and B. Kutuza, Radiotekh. Elektron. **23**, 1792-1806 (1978).
18. A. Evtushenko, G. Zagorin, B. Kutuza, A. Sobachkin, A. Hornbostel, and A. Schroth, Izvestiya - Atmospheric and Ocean Physics **38**, 470-476 (2002).
19. H. Czekala and C. Simmer, Journal of Quantitative Spectroscopy and Radiative Transfer **60**, 365-374 (1998).
20. A. Moroz, Applied Optics **44**, 3604-3609 (2005).
21. Y. A. Ilyushin and B. G. Kutuza, Proceedings - 2013 International Kharkov Symposium on Physics and Engineering of Microwaves, Millimeter and Submillimeter Waves, MSMW 2013 300-302 (2013).